

3D Reservoir Modelling and Hydrocarbon Volume Estimation of “X” Field, Niger Delta, Nigeria

Kenechukwu O. Ezebialu¹, Michael E. Ubituogwale¹, Eunice A. Odegua¹, Eric U. Eche², Anthony B. Sunebari²

¹Center of Excellence in Geosciences and Petroleum Engineering, University of Benin, Nigeria

²Centre for Petroleum Geosciences, University of Port Harcourt, Port Harcourt, Nigeria

Abstract-The field is prospective but largely underdeveloped as only four vertical wells have been drilled, leading to limited data and/or poor data quality. The aim of this study is to integrate cross-domain data to build a static reservoir model, estimate the in-place hydrocarbon volume and run an uncertainty analysis to validate the estimated volume. Available data include 3D seismic, well data and reservoir fluid properties. The integrated workflow includes petrophysical evaluation, seismic interpretation, facies definition, well correlation, static modelling, static volume estimation and uncertainty analysis. Three reservoirs, designated Reservoir 1, Reservoir 2 and Reservoir 3 were characterized in this project. Average porosity and permeability in the three reservoirs are approximately 30% and 100 millidarcy (mD) respectively. Reservoirs 1 and 3 are gas reservoirs while Reservoir 2 is an oil and gas reservoir. Static volume estimates in the three reservoirs are 1204 Billion Standard Cubic Feet (Bscf) and 308 Bscf of gas in Reservoirs 1 and 3 respectively, and 568 Million Stock Tank Barrel (MMstb) and 384 Bscf of oil and gas respectively in Reservoir 2. Uncertainty analysis was carried out using the Monte-Carlo sampling method in order to validate the estimated static volume in Reservoir 2. The results increased the level of confidence in the initial static volume estimates. Reservoir 2 was focused on due to the higher demand of oil.

I. INTRODUCTION

Reservoir modeling involves the construction of a computer model of a petroleum reservoir, for the purposes of improving estimation of reserves and making decisions regarding the development of the field and evaluating alternative reservoirs. Integrated reservoir models represent the most valuable technical approach for estimating the oil and gas reserves and computing profiles, reducing the uncertainties always associated with the reservoir volume and description. Considering the high investment associated with developing a reservoir, appropriate management of these subsurface uncertainties enhance the prediction of the subsurface volume, reduces time and improves the quality of key development decisions.

A. Regional Geology

The Niger Delta Basin is a wave dominated delta with tidal and fluvial influences - with the sediments typically sourced from the Benue and Niger River. Its subaerial exposure is about 300 km from apex to coast, spreading over about 75, 000 km², with two lobes protruding 250 kms into the deep waters [1]. The basin is pervaded with faults, some of which are large syn-sedimentary faults, which divide the basin into five (5) depobelts (Figure.2.2). These syn-sedimentary faults are mainly formed due to the mobility of the underlying over pressured marine shale (Akata Formation) which is overlain by deltaic sediments (Agbada Formation), and finally the continental deposits (Benin Formation) typically migrate southwards outbuilding the delta [2].

The depobelts of the Niger Delta represent cycles of deposition which are about 30-60 km wide, formed by the interdependencies of sediment supply and subsidence with a grossly southward progradation over the oceanic crust [3]. From oldest to youngest (North to South) the depobelts are the Northern Delta, Greater Ughelli, Central Swamp, Coastal Swamp and Offshore depobelts. The structural deformation of the Niger Delta shows extensional features at the Northern (onshore part), translation features in the middle and compression features offshore (Figure 2.3). This characteristic deformation forms the primary controls for hydrocarbon traps and accumulation in the basin as seen below; The Onshore Niger Delta hydrocarbons are trapped mainly by growth faults, roll over anticlines and collapsed crest structures which are characteristic of extension deformation. Offshore Niger Delta on the other hand is characterized by collapsed crests, back-to-back features and k-faults [4]. The consensus then is that, the structural deformation of the Niger Delta typically drives the dynamics of the basin and using this structural deformation, the basin can be subdivided into units that would be expected to have similar characteristics (fault pattern, hydrocarbon accumulation etc.).The stratigraphy of Niger Delta comprisesof;

- *Akata Formation*

This is composed mainly of marine shales, with sandy and silty beds which are thought to have been laid down as turbidites and continental slope channel fills. It is estimated that the formation is up to 7,000 meters thick (Doust and Omatsola, 1990).

- *Agbada Formation*

This is the major petroleum-bearing unit in the Niger Delta. The formation consists mostly of shoreface and channel sands with minor shales in the upper part, and alternation of sands and shales in equal proportion in the lower part. The thickness of the formation is over 3,700 meters.

- *Benin Formation*

This is about 280 metersthick but may be up to 2,100 meters in the region of maximum subsidence [5] and consists of continental sands and gravels. From the Eocene to the present, the delta has prograded south-westward, forming depobelts that represent the most active portion of the delta at each stage of its development [1]. “(see Figure 2.2) shows these depobelts that form one of the largest regressive deltas in the world with an area of some 300,000 km² [6], a sediment volume of 500,000 km³, and a sediment thickness of over 10 km in the basin depocenter.

II. METHODOLOGY

Thisgives a detailed procedure used to build the static (earth) model of the three reservoirsof interest, and the estimation of in-place hydrocarbon volumes;

1. Evaluation of petrophysical properties from well logs.
2. Fault and horizon interpretation from 3D-seismic.
3. Establishmentof stratigraphic equivalence/framework by correlating the reservoir tops across thefour wells.
4. Building of a 3D static reservoir model for all the three reservoirs of interest via structural andproperty modelling.
5. Estimate in-place hydrocarbon volumes and perform uncertainty analysis.

A Workflow

The 3D reservoir model requires input from Geophysics, Geology and Petrophysics. The static model in turn serves as input for the Reservoir Engineer (RE) to build the dynamic model (see figure 1).

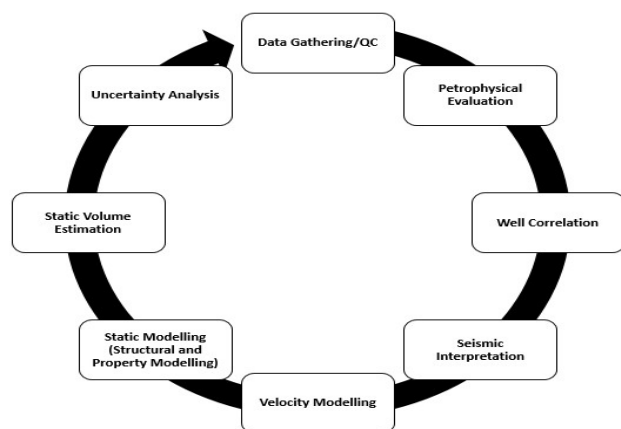


Figure 1: showing integrated workflow

B Project Set-Up

A new project was created in Petrel and the Coordinate Reference System (CRS) for the “X” field was selected. The option “Field units” was selected as the unit system in accordance with the units in the dataset, that is, Depth in Feet, Area in Acres, Volume in Acre.ft, STOIP in MMstb, GIIP in Bscf, etc.

C Facies Definition

The term “facies” was introduced by the Swiss geologist AmanzGressly[7]. Facies refers to a unique body of rock (bed/laminae), characterized by distinct petrographic properties (grain size, color, sorting, thickness, physical properties and biogenic features); facies are interpreted in terms of the processes of sedimentation because it is unique to a depositional environment [8]. The uniformity of physical properties means uniform reservoir properties; facies form the fundamental building block for describing sedimentary rocks [8].

Lithofacies refers to facies’ description based on lithology. Lithofacies constitute the smallest building block in reservoir models. In the absence of core data, petrophysical properties obtained from logs such as gamma-ray (GR), porosity and permeability, can be used to define lithofacies.

In this project, the well calculator in Petrel was used to calculate the lithofacies for all four wells, using the GR log as the criterion. Thus, three lithofacies namely, sand, silt and shale, were generated. The GR log motif trend was used to define the facies based on depositional environment (see figure 2)

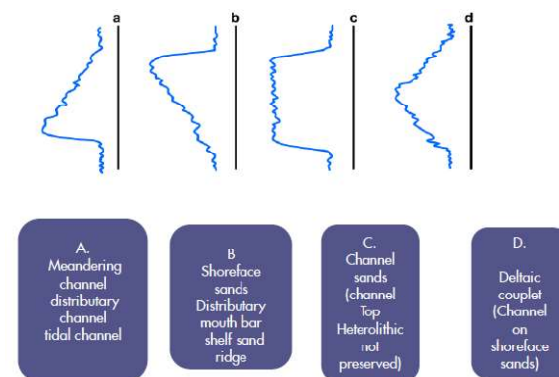


Figure 2: Idealized GR log motif trend for different depositional environments [9]

D Well Correlation

The lithostratigraphic method was employed for well correlation in this study. After defining the lithofacies log, a W-E cross-section was taken across the four wells (see figure 3). The wells were correlated along strike via this cross-section. The imported well tops were adjusted to the top of the sand across the four wells. The sand or reservoir tops were then matched from one well to another, effectively creating a stratigraphic framework of the field. Correlation from one

well to another establishes stratigraphic equivalence between their units. Three well tops were correlated, and they correspond to the three modelled reservoirs.

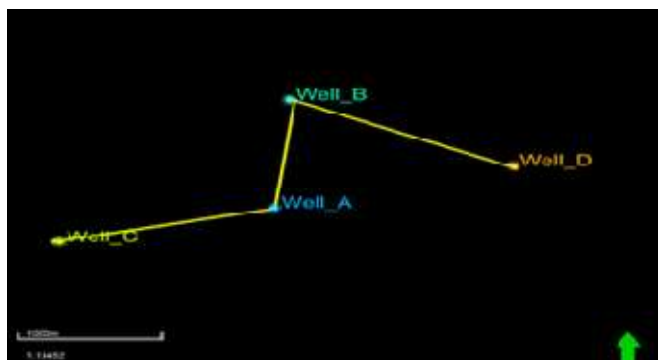


Figure 3: The W-E cross-section across the four wells

E Static Reservoir Modelling

Static or geological modelling is a dual process involving bringing together the structural and property models to form a single model. Structural modelling in turn comprises three main aspects— fault modelling, horizon modelling and 3D gridding (see figure 4). Property modelling also comprises facies modelling and petrophysical modelling.

- *Structural Modelling*

The depth-converted fault sticks and surfaces generated by the Geophysicist serve as input in the structural model. The surfaces are six in total, i.e. the three reservoir tops and their respective bases. The method used for structural modelling in this project is corner point gridding. The structural modelling workflow using corner point gridding is summarized thus (see figure 4). Each step in the corner point gridding method used is outlined and discussed in detail below.

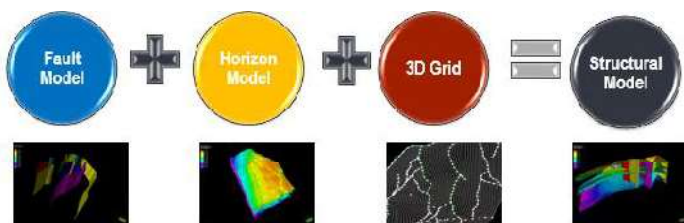


Figure 4: showing Structural modelling aspects

- *Fault Modelling:*

The model in which the fault pillars will be stored was first defined. Fault pillars were then generated from the fault sticks, ensuring that only few of the fault sticks were selected as fault pillars. However, enough fault sticks were selected in order to preserve the general shape of the faults. The listric fault pillar geometry was selected due to the nature of the interpreted faults in the field. After fault pillar generation, the top surface of Reservoir 1 and the base surface of Reservoir 3 were used to cut or restrict the fault pillars to the interval of interest. The resultant fault pillars have three shape points— the top, mid and base shape points. The faults

were subsequently modelled, converting the fault pillars to fault planes. The model boundary was defined, using the major growth fault as the northernmost boundary and the limits of the top surface as the edge boundaries. The defined boundary further constricted the model to the area of interest. After running the pillar gridding, three skeleton grids were generated— top, mid and base skeleton grids. Each skeleton grid is attached to the top, mid and base shape points of the fault pillars (see figure 5). These pillars serve to connect every corner of every grid cell on one skeleton grid to a corresponding corner on an adjacent skeleton grid (see figure 6). Before proceeding, it was necessary to quality check the mid skeleton grid in order to fix problems such as twisted cells, peaks and envelopes in the grid. The mid skeleton grid was focused on because the top and base skeleton grids are extrapolations of the mid skeleton grid

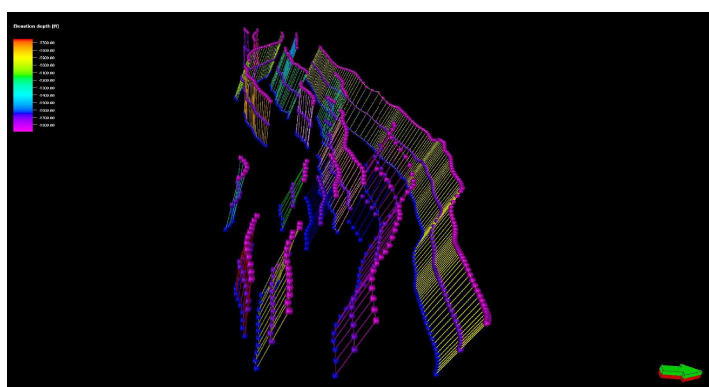


Figure 5: Fault pillars used for fault modelling

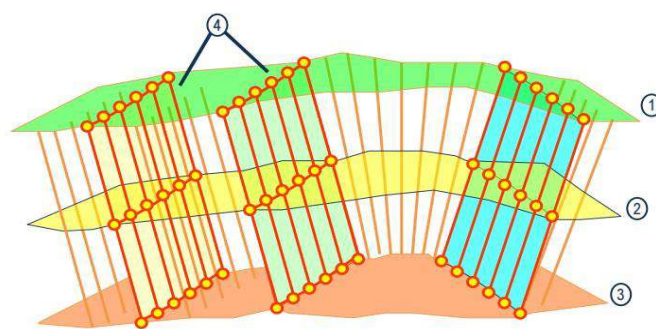


Figure 6: Top, mid and base skeleton grids (labelled 1, 2, 3), and the pillars between the faults [10]

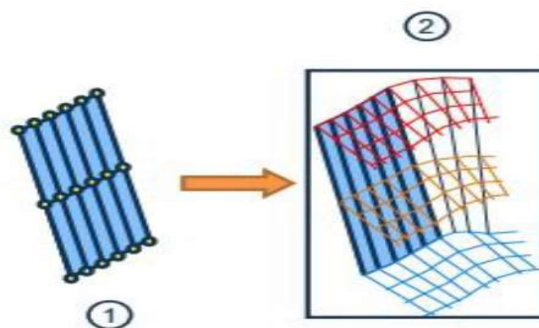


Figure 7: Progressing to pillar gridding after fault modelling [10]

- *Horizon Modelling, Zoning and Layering*

At this stage, the depth-converted horizons/surfaces were inserted into the 3D grid, producing horizon models fitting the defined model boundary. The pillars served to define the framework (including faults and grid cell size) into which the horizons/surfaces were inserted. The modelling of six horizons automatically created five zones in the model—three reservoir zones and two shale zones separating the reservoir zones. Fifty layers were then created per reservoir. The choice of number of layers was informed by the resolution of the GR log as defined by its motif.

The structural modelling method employed ultimately created a structural 3D grid housing the three reservoirs. However, the grid cells are all empty at this stage. Since empty grid cells are not representative of true subsurface conditions, the need arises to solve this problem. This is where property modelling comes in.

- *Property Modelling*

Property modelling is the process of populating the empty grid cells with facies (discrete log) and petrophysical properties (continuous log), thus creating a model more representative of the subsurface. Here, the defined lithofacies log created by the Geologist and the petrophysical properties generated in Techlog by the Petrophysicist, come in handy. Figure 8 summarizes the property modelling workflow. The steps in the property modelling workflow are discussed in detail below.

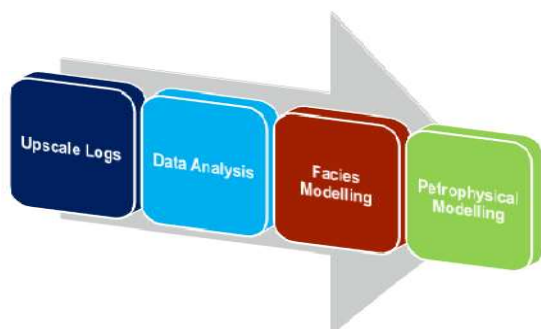


Figure 8: Property modelling workflow

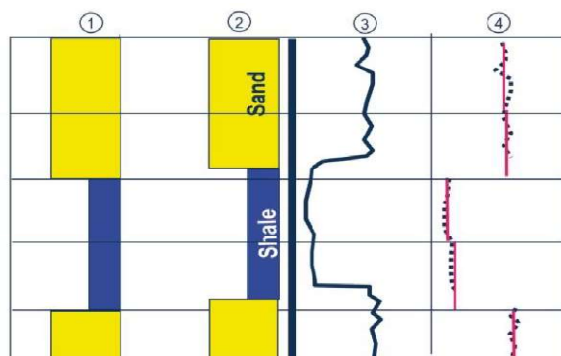


Figure 9: Result of biasing petrophysical properties to facies: (1) Up-scaled facies, (2) Raw facies, (3) Raw porosity, (4) Up-scaled porosity [11]

- *Upscale Logs*

To achieve this, all the generated petrophysical logs including porosity, permeability, volume of shale (Vsh) and water saturation, were imported into Petrel. The lithofacies and petrophysical logs were then upscaled in order to reduce or equate their resolution to that of the grid cells, making it coarser. The lithofacies log was upscaled using the “most of” averaging method, suitable for discrete logs. The “most of” method uses the most represented value to populate the grid cell. The petrophysical logs were upscaled using the “arithmetic” averaging method and were all biased to the lithofacies. This biasing was done to ensure that the up-scaled petrophysical values are a better match for the up-scaled facies (see fig.9).

- *Data Analysis*

At this stage, data analysis was carried out for both the facies and petrophysical properties. This involved variogram analysis. A variogram is used to model the way in which two values in space or time are correlated, giving a quantitative description of the variation in a property as a function of the separation distance between data points (Petrel Property Modelling, 2017). The variogram analysis workflow as outlined in Petrel Property Modelling (2017) is shown below:

- Determine the directions of the variogram analysis (usually three directions orthogonal to each other— vertical, major and minor).
- Calculate an experimental variogram for each direction
- Create a variogram model fitted to the experimental variogram in each direction

The experimental variogram refers to the sample points or sample variogram, while the fitted curve is the variogram model (see fig. 10). As hinted before, variogram models are built for each direction. The vertical variogram is easily estimated due to the plethora of data obtained from high-resolution well logs. The reverse is the case for the horizontal variogram model (major and minor directions) because there is limited data in the horizontal direction. The variogram model for each direction will determine how the properties will vary from one point to another. It therefore will determine the distribution of facies and petrophysical properties from the wells to the rest of the field.

Three variogram model types are available in Petrel— Spherical, Exponential and Gaussian. The spherical variogram model type was used for both facies and petrophysical properties in this project, due to its relative simplicity. Variogram models were generated for the sand, silt and shale facies respectively and likewise for each petrophysical property. Variogram ranges in the major and minor directions were obtained from the variogram map of the facies or petrophysical properties, while the vertical variogram range was determined by the variogram model (labelled “4” in

Figure 3.12). Azimuth values were also obtained from the variogram maps.

- *Facies Modelling*

The facies were modelled using Sequential Indicator Simulation (SIS), a stochastic pixel-based algorithm. Stochastic techniques are typically used in areas of sparse data. The SIS algorithm was therefore chosen for this project because of the limited number of wells in the field.

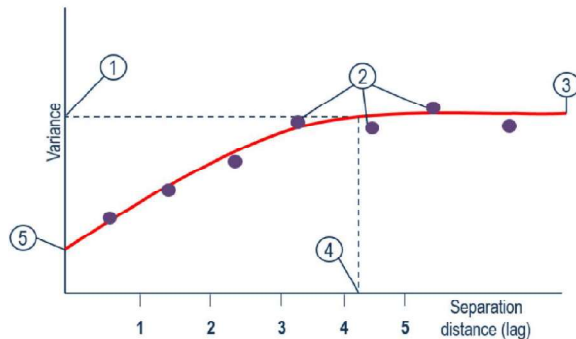


Figure 10: Experimental variogram: (1) Sill, (2) Sample variogram, (3) Variogram model, (4) Vertical range, (5) Nugget [11].

Stochastic				
Pixel based				Object based
Sequential Indicator Simulation and Sequential Indicator Simulation (Gslib)	Truncated Gaussian Simulation	Truncated Gaussian Simulation with trends	Multi-point Facies Simulation	Object Modeling • General object • Fluvial • Adaptive
Honors input distribution and directional settings such as variograms and trends.	Used where facies are known to be sequential. Honors input data, global fractions, and trends.	Distributes facies based on transition between facies and trend direction (converted into probabilities).	A training image describes the spatial correlation from one-to-multiple points (for facies and their relative position).	Allows population of a discrete facies model with different bodies of various geometries, facies, and fractions.

Figure 11: Stochastic algorithms in Petrel [11]

- *Petrophysical Modelling*

After facies modelling, the petrophysical properties namely, porosity, permeability and volume of shale were modelled using the Gaussian Random Function Simulation (GRFS) algorithm. This is also a stochastic technique. It was employed here also because of the limited number of wells. The petrophysical models are constrained by the facies model because they were earlier biased to the facies during up-scaling.

After this, the hydrocarbon contacts obtained from the Petrophysicist were modelled in Petrel. With the help of the Reservoir Engineer, a Saturation Height Function (SHF) was generated using the calculator in Petrel. Inputs in this function are the lithofacies, reservoir zone hierarchy (a number assigned to each reservoir zone) and the contact values. The saturation height function was used to create the Saturation Height Model (SHM) which is the water saturation model.

F Static Volume Estimation

The contacts were used as input for the volume estimation. GWC occurs at 5963 ft. and 6481 ft. in Reservoirs 1 and 3 respectively, while GOC and OWC occur at 6205 ft. and 6325 ft. respectively in Reservoir 2. Thus, Reservoirs 1 and 3 are gas reservoirs while Reservoir 2 contains oil and gas.

The Stock Tank Oil Initially in Place (STOIP) was calculated using the formula below.

$$STOIP = 7758 * Ah\phi * NTG * (1 - Sw) / Boi \quad (3.1)$$

Likewise, the Gas Initially in Place (GIIP) was calculated using the below formula.

$$GIIP = 43560 * Ah\phi * NTG * (1 - Sw) / Bgi \quad (3.2)$$

Where:

Ah = Gross rock volume (in acre.ft)

A = Drainage area (in acre)

h = Reservoir thickness (in ft.)

ϕ = Porosity

NTG = Net-To-Gross

Sw = Water saturation

Boi = Initial oil formation volume factor (in rb/stb)

Bgi = Initial gas formation volume factor (in cf/scf)

STOIP is measured in stock tank barrel (stb) while GIIP is measured in standard cubic feet (scf).

The Boi and Bgi were obtained from the Reservoir Engineer, although only for Reservoir 2. Due to time constraint, the team decided to focus on Reservoir 2. Therefore, reservoir simulation was performed only for Reservoir 2. For this reason, the Bgi obtained from Reservoir 2 was also used for both Reservoir 1 and 3. The Reservoir Engineer also provided the recovery factor which when multiplied with the STOIP, gave the recoverable volume of oil. The recovery factor was also estimated for Reservoir 2 alone.

G Uncertainty Analysis

Uncertainties in the hydrocarbon in-place volume was analyzed for Reservoir 2 using the “Uncertainty and Optimization” function in Petrel. First, the base case for Reservoir 2 was selected and dropped into the uncertainty analysis dialog box. Petrophysical properties, lithofacies and contacts were then selected for use in the uncertainties computation. Normal distribution was used for the GOC and OWC, the GOC value was inputted as the mean, and a standard deviation of 30 was selected. The Monte-Carlo sampling method was selected, and 50 samples were subsequently run. The higher the number of samples run, the greater the likelihood of accuracy in the results. The results were displayed on a histogram window, and the most likely scenario (P50), which represents the base case scenario was

selected. P10 and P90 represent the low and high case respectively, i.e. the pessimistic and optimistic scenarios. The STOIP and GIIP in the base case (P50) were observed to be close to the values obtained from static volume estimation, thus validating the static volume estimates.

III. RESULTS AND DISCUSSION

A Facies Definition

Three lithofacies were defined using the GR log as the criterion— sand, silt and shale. The motif trend of the GR log was also used to define the facies in the field based on depositional environment as upper shoreface sands, lower shoreface sands and marine shales (see fig. 12). The shoreface sands belong in the delta front.

B Upper Shoreface Sands

These are recognized by a prograding or coarsening upward GR log trend, very low volume of shale and a very narrow separation of the neutron-density logs. They have the least volume of shale amongst all the facies identified in the field. These characteristics are indicative of clean sands which can serve as excellent oil and gas reservoirs. The upper and lower shoreface sands as a unit make up the reservoir in the field. These upper shoreface sands belong in the delta front section of the prograding wave-dominated Niger Delta, occurring from fair weather wave base to low tide.

C Lower Shoreface Sands

These are also recognized by a prograding, funnel-shaped or coarsening upward GR log trend and are overlain by the upper shoreface sands. Their neutron-density log separation is wider than that of the upper shoreface sands. Being less clean, they have higher volume of shale and silt input than the upper shoreface sands. These sands are generally finer grained and consequently less permeable than their upper shoreface counterparts. They are good reservoirs and belong in the delta front of the prograding Niger Delta, occurring below fair-weather wave base.

D Marine Shales

These are easily recognized by their high readings on the GR log. They are also characterized by their large positive neutron-density log separation. These shales represent condensed zones formed during marine flooding events. They form the zones which separate one reservoir from another, effectively sealing the reservoirs.

E Well Correlation

Matching the tops of all three reservoirs across the four wells gives an idea of the stratigraphic framework of the reservoir model. The correlation along strike is shown in Fig.13.

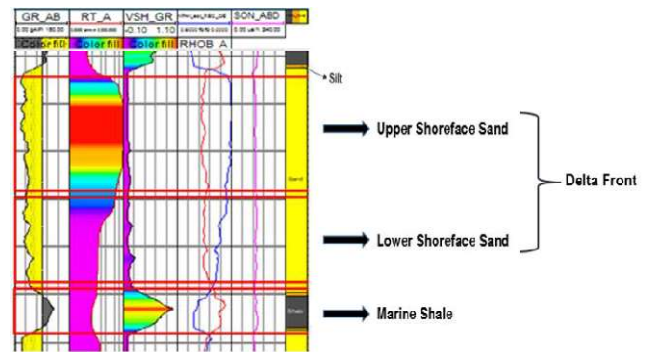


Figure 12: Facies defined using the GR and VSH log

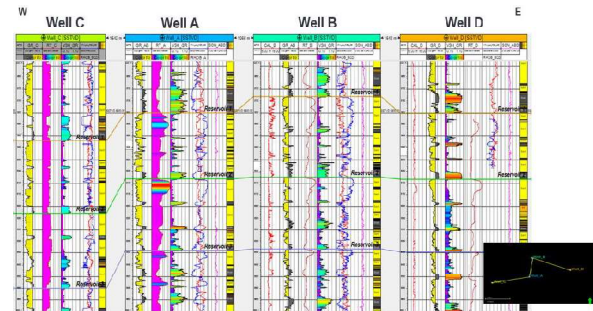


Figure 13: Correlation across the four wells (inset: W-E cross-section in 2D)

F Static Reservoir Modelling

Here the results obtained from structural and property modelling are presented. The structural and property models (the static model) determine the estimated volumes of in-place hydrocarbon in the three reservoirs.

G Structural Modelling

The fault model, horizon model and 3D grid constitute the structural model. The structural model partly determines the in-place hydrocarbon volumes found in structural traps in the reservoirs. The results obtained from structural modelling are shown in the figures below.

Figure 14 shows the major growth fault which was used to define the northernmost boundary of the model. The modelled faults are mostly synthetic though some antithetic faults also occur. The faults are all listric normal faults as expected in this area of the Niger Delta basin. The fault and horizon framework (Figure 15) show how the horizons terminate on the faults to form simple rollover structures typical of the Niger Delta. Figure 16 show the resultant structural 3D grid with the three reservoir zones (the thicker zones) separated by thinner shale zones. Each reservoir zone is further subdivided into fifty layers.

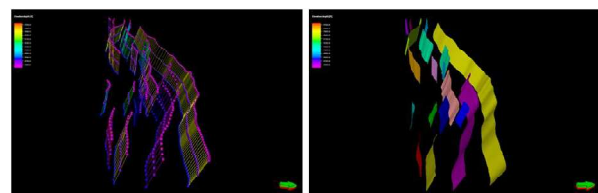


Figure 14: The fault pillars and fault model

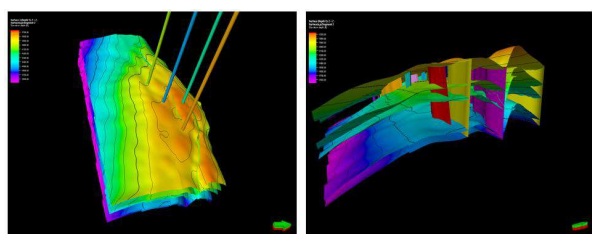


Figure 15: The modelled horizons and fault framework

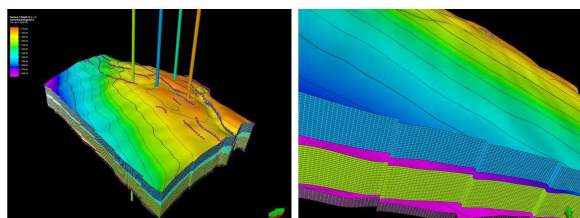


Figure 16: The structural 3D grid and layering

H Property Modelling

This comprises the facies model and petrophysical models. The petrophysical models are the porosity, permeability, volume of shale and water saturation models. The property model also determines the in-place hydrocarbon volumes found in the reservoirs, especially in stratigraphic traps. Table 1 shows the summary of the petrophysical properties obtained from the Petrophysicist and used by the Geologist for property modelling.

Table 1: Summary of petrophysical properties

Zones	Average Shale Volume (v/v)	Net to Gross	Average Porosity (v/v)	Average Water Saturation (v/v)	Average HC Saturation (v/v)	Contacts (ft.)
Reservoir 1	0.077	0.848	0.259	0.411	0.588	5963 (GWC)
Reservoir 2	0.088	0.833	0.263	0.347	0.652	6205 (GWC) 6325 (OWC)
Reservoir 3	0.093	0.931	0.263	0.461	0.538	6481 (GWC)

The results obtained from variogram analysis which determined the distribution of facies and petrophysical properties in the model are shown in the tables below.

Table 2: Variogram ranges used for facies modelling

Reservoir 1 (Zone 1)				
Facies	Major range	Minor range	Vertical range	Azimuth
Shale	2188.90	1337.90	13.59	140.00
Silt	1952.20	1351.00	10.87	157.00
Sand	2092.53	1953.69	10.75	123.00

Reservoir 2 (Zone 2)				
Facies	Major range	Minor range	Vertical range	Azimuth
Shale	1383.36	1171.00	26.19	140.00
Silt	1948.20	1382.00	14.60	157.00
Sand	1457.00	1351.00	26.00	123.00

Reservoir 3 (zone 3)				
Facies	Major range	Minor range	Vertical range	Azimuth
Shale	2549.80	1321.60	5.60	140.00
Silt	1811.50	1330.00	4.80	157.00
Sand	1461.00	1326.90	3.30	123.00

Table 3: Variogram ranges used for porosity modelling

Reservoir 1 (Zone 1)				
Facies	Major range	Minor range	Vertical range	Azimuth
Shale	2002.90	1618.60	11.55	140.00
Silt	1996.80	1385.00	5.36	157.00
Sand	1367.70	1339.70	24.30	123.00

Reservoir 2 (Zone 2)				
Facies	Major range	Minor range	Vertical range	Azimuth
Shale	1353.60	1278.00	5.90	140.00
Silt	1859.90	1241.00	3.70	157.00
Sand	1235.40	1222.50	29.30	123.00

Reservoir 3 (zone 3)				
Facies	Major range	Minor range	Vertical range	Azimuth
Shale	814.20	807.20	3.98	140.00
Silt	1390.20	698.70	1.90	157.00
Sand	1224.00	1224.00	4.90	123.00

Table 4: Variogram ranges used for permeability modelling

Reservoir 1 (Zone 1)				
Facies	Major range	Minor range	Vertical range	Azimuth
Shale	1942.60	1808.20	8.40	140.00
Silt	1913.54	1478.69	5.36	157.00
Sand	1905.90	1646.50	24.80	123.00

Reservoir 2 (Zone 2)				
Facies	Major range	Minor range	Vertical range	Azimuth
Shale	1210.40	1172.60	6.20	140.00
Silt	2030.20	1375.40	5.80	157.00
Sand	1991.27	1587.73	20.83	123.00

Reservoir 3 (zone 3)				
Facies	Major range	Minor range	Vertical range	Azimuth
Shale	2181.80	1937.60	4.70	140.00
Silt	1824.63	1758.41	1.63	157.00
Sand	1758.41	1325.14	5.60	123.00

Table 5: Variogram ranges used for volume of shale modelling

Reservoir 1 (Zone 1)				
Facies	Major range	Minor range	Vertical range	Azimuth
Shale	1626.65	1329.84	5.40	140.00
Silt	2032.80	1342.40	2.89	157.00
Sand	1769.41	1395.18	24.47	123.00

Reservoir 2 (Zone 2)				
Facies	Major range	Minor range	Vertical range	Azimuth
Shale	1957.18	1715.22	8.45	140.00
Silt	2105.38	1381.67	5.48	157.00
Sand	1363.21	1363.21	17.32	123.00

Reservoir 3 (zone 3)				
Facies	Major range	Minor range	Vertical range	Azimuth
Shale	2472.50	2035.42	5.65	140.00
Silt	2045.06	1328.83	1.71	157.00
Sand	2264.27	1318.87	8.89	123.00

The facies model clearly shows the distribution of sand, silt and shale in the three reservoirs. Due to the high net-to-gross values for each reservoir (Table 1), the volume of sand in the model is very high (Figure 17). The distribution is however determined by the stochastic Sequential Indicator Simulation (SIS) technique used. The modelled porosity is effective porosity, i.e. the volume of interconnected pores. The porosity model shows more variability in distribution compared to the facies model (Figure 18). The porosity in the model ranges from around 15% to 35%. Most of the porosity is around 30%. This indicates good porosity capable of housing considerable hydrocarbon volumes.

The permeability in the model ranges from around 10 mD to around 100 mD, with the majority being close to 100 mD (Figure 4.10). This indicates good permeability in the reservoirs. Each reservoir has low volume of shale due to their high net to gross values. From Table 4.1, the volume of shale for Reservoir 1 can be estimated as 23%, Reservoir 2 as 12% and Reservoir 3 as 7%. The average volume of shale for all three reservoirs is therefore 14%, which is quite low.

As mentioned in chapter three, a Saturation Height Function (SHF) obtained from the Reservoir Engineer was used to build a Saturation Height Model (SHM) which serves as the water saturation model. The water saturation model was limited to the zones above contact by including a filter in the model which gives a water saturation value of 1 (100%) to all areas below the contact (Figure 21). The contacts obtained from the Petrophysicist (Table 1) were modelled in Petrel and are shown in Figure 22.

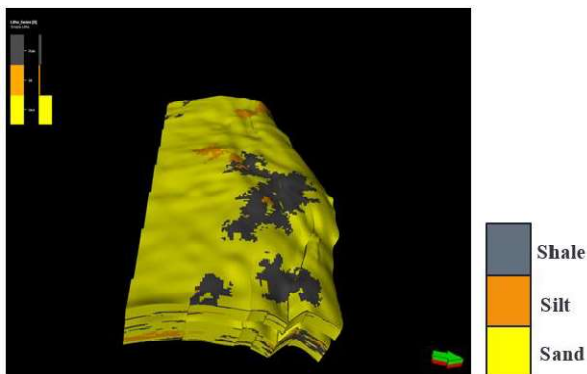


Figure 17: The facies model

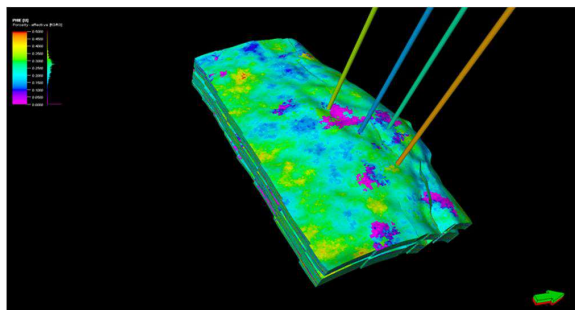


Figure 18: The porosity model

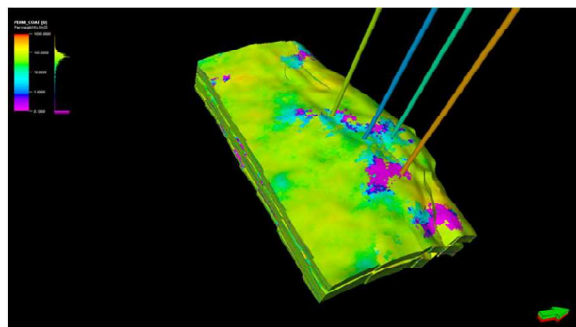


Figure 19: The permeability model

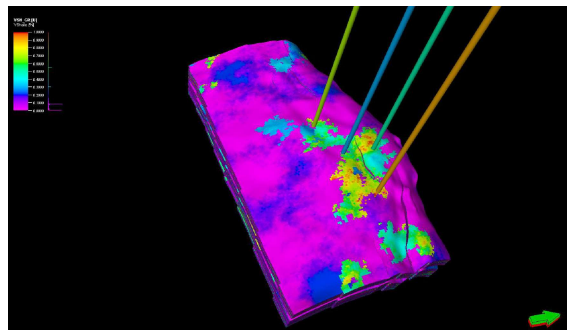


Figure 20: The volume of shale model

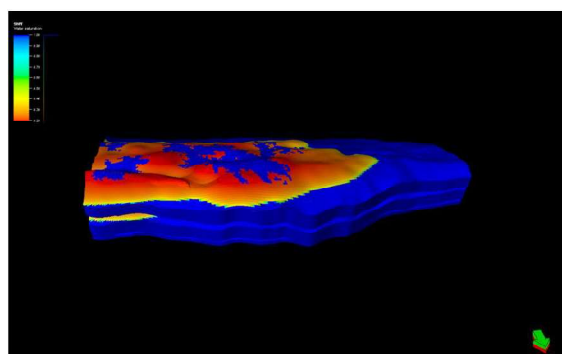


Figure 21: The water saturation model

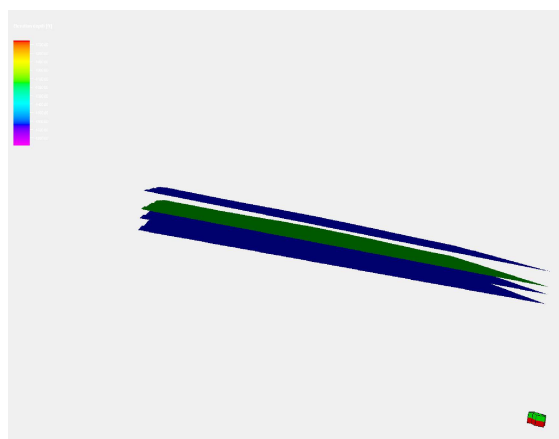


Figure 22: The modelled contacts from top to bottom: GWC for Reservoir 1, GOC for Reservoir 2, OWC for Reservoir 2, and GWC for Reservoir 3

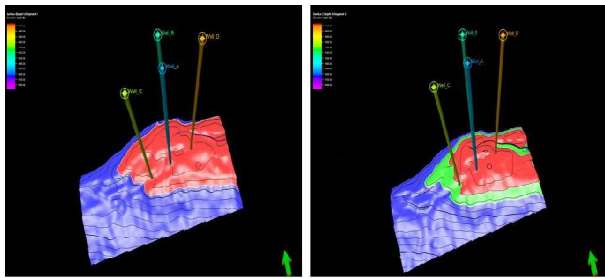


Figure 23: Top surface of Reservoir 1 and the GWC and top surface of Reservoir 2 and the GOC and OWC

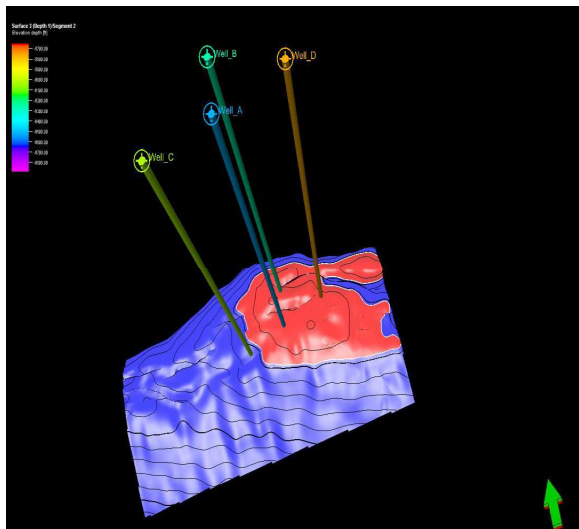


Figure 24: Top surface of Reservoir 3 and the GWC

4.4 Static Volume Estimation

As stated in chapter three, Reservoirs 1 and 3 are gas reservoirs, while Reservoir 2 contains both oil and gas. The respective static volumes estimated for each reservoir are shown in Table 4.6 below. The bulk and net reservoir volume are the same because effective porosity was used to define the bulk volume, implying a net-to-gross value of 1. Since only Reservoir 2 was simulated by the Reservoir Engineer, Boi and Bgi were available only for this reservoir. The Boi and Bgi gotten from the Reservoir Engineer for Reservoir 2 are 1.153 rb/stb and 1.297 rb/Mscf respectively. This Bgi value was also used to calculate the GIIP for Reservoirs 1 and 3.

Table6: The estimated static volumes in all three reservoirs

	Bulk volume (*10 ⁶ ft ³)	Net volume (*10 ⁶ ft ³)	Pore volume (*10 ⁶ RB)	HCPV oil (*10 ⁶ RB)	STOIP (in oil) (*10 ⁶ STB)	HCPV gas (*10 ⁶ RB)	GIIP (in gas) (*10 ⁶ MSCF)
Reservoir 1	35578	35578	1641	N/A	N/A	1562	1204
Reservoir 2	47040	47040	1876	655	568	498	384
Reservoir 3	9758	9758	457	N/A	N/A	400	308

I Uncertainty Analysis

The uncertainty analysis was carried out on hydrocarbon in-place volumes in Reservoir 2. The results are displayed in the histograms below.

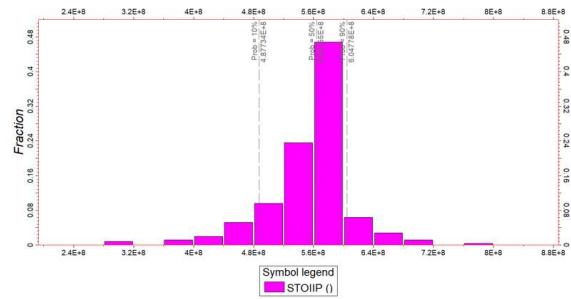


Figure 4.17: Histogram showing low, base and high case of STOIP

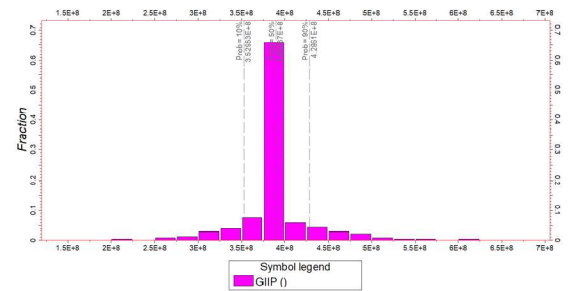


Figure 4.18: Histogram showing low, base and high case of GIIP

The histograms show low, base and high cases for both STOIP and GIIP. The low case (P10) corresponds to the pessimistic scenario, the base case (P50) corresponds to the most likely scenario, and the high case (P90) corresponds to the optimistic scenario. The base case was selected for both the STOIP and GIIP. The base case of STOIP and GIIP are 564 MMstb and 390 Bscf respectively. Table 4.7 shows the changes in hydrocarbon in-place volumes after uncertainty analysis.

Table7: Static volume changes after uncertainty analysis

	Before Uncertainty Analysis	After Uncertainty Analysis	Difference	% Difference
STOIP (MMstb)	568	564	4	0.70
GIIP (Bscf)	384	390	6	1.56

From Table 4.7 above, the STOIP and GIIP do not change significantly after uncertainty analysis. This validates and increases the level of confidence in the initial static volume estimates.

IV. CONCLUSIONS

The following conclusions can be made from the integrated 3D reservoir modelling of the “X” field:

Consistent with known Niger Delta structures, a major regional growth fault, synthetic and antithetic faults, collapsed crest structures, and roll over anticlines were identified in the field.

Three facies were defined based on lithology— sand, silt and shale. Facies were also defined as upper shoreface, lower shoreface and marine shales based on environment of deposition.

Average porosity in the three reservoirs is approximately 30%.

Average permeability in the three reservoirs is approximately 100 mD.

In-place hydrocarbon volumes estimated are 1204 Bscf of gas in Reservoir 1, 568 MMstb of oil and 384 Bscf of gas in Reservoir 2, and 308 Bscf of gas in Reservoir 3.

Uncertainty analysis carried out on hydrocarbon in-place volumes in Reservoir 2, shows that there are minimal changes in static volumes after uncertainty analysis, thus increasing the level of confidence in the initial static volume estimates.

REFERENCES

- [1] Doust, H. and Omatsola, E.M. (1990). Niger Delta. In: J. D. Edwards and P.A. Santogrossi (eds.), *Divergent/Passive Margin Basins. AAPG Memoir 48*: 239-248.
- [2] Knox, G.J. and Omatsola, E.M. (1989). Development of the Cenozoic Niger Delta in terms of the "Escalator Regression" Model and Impact on Hydrocarbon Distribution. *Proceedings KNGMG Symposium "Coastal Lowlands, Geology and Geotechnology", 1987*: Dordrecht, Kluwer, p. 181-202.
- [3] Stacher, P. (1995). Present Understanding of the Niger Delta Hydrocarbon Habitat. In: M.N. Oti and G. Postma (eds.), *Geology of Deltas*: Rotterdam, A.A. Balkema, p. 257-267.
- [4] Doust, H. and Omatsola, E.M. (1989). Niger Delta. *AAPG Memoir 48*: 201-238.
- [5] Whiteman, A. (1982). *Nigeria: Its Petroleum Geology, Resources and Potential*. Graham and Trotman, London, p. 381.
- [6] Kulke, H. (1995). Nigeria. In: H. Kulke (ed.), *Regional Petroleum Geology of the World, Part II: Africa, America, Australia and Antarctica*. GebruderBorntraeger, Berlin, p. 143-172.
- [7] Cross, T.A. and Homewood, P.W. (1997). AmantzGressly's Role in Founding Modern Stratigraphy. *Geological Society of America Bulletin, 109*: 1617-1630.
- [8] Ladipo, K.O. (2017). *CoE Lecture Notes: Applied Stratigraphy and Sedimentology*.
- [9] Kakayor, G.O. (2013). *CoE Lecture Notes: Reservoir Description and Characterization*, p. 20.
- [10] Schlumberger (2018). *Structural Modelling: Training and Exercise Guide, Version 2017*.
- [11] Schlumberger (2017). *Property Modelling: Training and Exercise Guide, Version 2017*.

APPENDIX

1	Acronym	Meaning
2	STOIP	Stock Tank Oil Initially in Place
3	MMstb	Million stock tank barrel
4	GIIP	Gas initially in place
5	Bscf	Billion standard cubic feet
6	Vsh	Volume of shale
7	GOC	Gas/Oil contact
8	OWC	Oil/Water contact
9	mD	MilliDarcy
10	Boi	Oil initial formation volume factor
11	Bgi	Gas initial formation volume factor
12	Rb/stb	Reservoir barrels/stock tank barrel
13	Rb/Mscf	Reservoir barrels/Million standard cubic feet